

# Imaging Features of Aggressive Giant Cell Tumors of the Mobile Spine: Retrospective Analysis of 101 Patients From Single Center

Bei Yuan, MD<sup>1,2</sup> , Lihua Zhang, MD<sup>3</sup>, Shaomin Yang, MD<sup>4</sup>, Hanqiang Ouyang, MD<sup>1</sup>, Songbo Han, MD<sup>3</sup>, Liang Jiang, MD<sup>1</sup>, Feng Wei, MD<sup>1</sup>, Huishu Yuan, MD<sup>3</sup>, Xiaoguang Liu, MD<sup>1</sup>, and Zhongjun Liu, MD<sup>1</sup>

Global Spine Journal  
2022, Vol. 12(7) 1449–1461  
© The Author(s) 2021  
Article reuse guidelines:  
sagepub.com/journals-permissions  
DOI: 10.1177/2192568220982280  
journals.sagepub.com/home/gsj



## Abstract

**Study Design:** Retrospective study.

**Objectives:** Giant cell tumors (GCTs) of the mobile spine can be locally aggressive. This study described and classified the typical and atypical appearance of aggressive spinal GCTs according to imaging findings to help the imaging diagnosis, especially for patients with rapid neurological deficit that may require emergent surgery without biopsy.

**Methods:** Computed tomography (CT) and magnetic resonance imaging (MRI) scans of patients diagnosed with aggressive spinal GCTs at single center were reviewed.

**Results:** Overall, 101 patients with 100 CT images and 94 MR images were examined. All lesions were osteolytic with cortical destruction; 95 lesions showed epidural extension; 90 were centered in the vertebral body; 82 showed pathological fracture and/or collapse of the vertebral body; 78 had pseudotrabeculation on CT; 80 showed low-to-iso signal intensity or heterogeneous high-signal intensity with cystic areas on the T2-weighted images; 9 showed fluid–fluid level on T2-weighted images; and 61 patients showed marked enhancement on contrast-enhanced CT and/or MRI. Forty-one lesions (40.6%) had at least 1 atypical radiographic feature: 19 involved  $\geq 2$  segments; 11 were centered in the posterior neural arch; 10 had a paravertebral mass over 2 segments; 16 showed partial margin sclerosis with partial cortical destruction on CT scans; and 3 showed mineralization within the tumor on CT. Eighty-eight patients underwent CT-guided biopsy with a diagnostic accuracy rate of 94.3%.

**Conclusions:** Spinal GCTs might appear more radiologically atypical, and about 40% of the lesions may have at least 1 atypical feature. CT-guided biopsies are recommended for definitive diagnosis.

## Keywords

giant cell tumor, spine, atypical, imaging features

## Introduction

Giant cell tumors (GCTs) of the bone are relatively common primary benign bone tumors, accounting for approximately 5% of all primary bone tumors in Western populations<sup>1</sup> and 20% in East Asian populations.<sup>2</sup> GCTs most frequently occur in young adults aged between 20 and 40 years, originating in the metaphyseal-epiphyseal area, with 70%-80% of GCTs being active lesions (Enneking Stage 2 [S2]).<sup>3,4</sup> On radiographs, they are typically eccentric, well-defined geographic lucent lesions with a non-sclerotic rim, centered in the metaepiphysis and extending into the subarticular bone.<sup>5</sup>

<sup>1</sup> Orthopaedic Department, Peking University Third Hospital, Haidian District, Beijing, China

<sup>2</sup> Peking University Health Science Center, Haidian District, Beijing, China

<sup>3</sup> Department of Radiology, Peking University Third Hospital, Haidian District, Beijing, China

<sup>4</sup> Department of Pathology, Peking University Third Hospital, Haidian District, Beijing, China

### Corresponding Authors:

Liang Jiang and Zhongjun Liu, Orthopaedic Department, Peking University Third Hospital, No. 49 North Garden Road, Haidian District, Beijing 100191, China.

Emails: jiangliang@bjmu.edu.cn; liuzj@bjmu.edu.cn



The incidence of GCTs in the mobile spine is 1.4%-9.4%.<sup>6</sup> Most spinal GCTs are aggressive (Enneking Stage 3 [S3]) and may involve soft-tissue masses extending into the spinal canal, which might lead to rapid neurological deficit and might require emergent surgery.<sup>6-8</sup> Furthermore, the accuracy of computed tomography (CT)-guided biopsy is about 61-93%.<sup>9-11</sup> In this circumstance, radiological features are very important, especially when a percutaneous biopsy is not available or misleading. According to their radiological features, spinal GCTs might appear more atypical than GCTs in the extremities and could lead to misdiagnosis.<sup>6,12</sup> Atypical manifestations of spinal GCTs include lesions located in the neural arch, involving more than 1 vertebra segment and/or over 2 segments of paraspinal soft tissue mass, and presence of partial sclerotic margins with partial cortical destruction.<sup>12-15</sup>

There are few in-depth reports of radiographic features associated with aggressive GCTs of the mobile spine, which limited to case reports or a few examples,<sup>15-17</sup> and there is no systematic summary of the atypical imaging features of spinal GCT. Since extensive knowledge of radiological features associated with spinal GCTs is important for clinical diagnosis, especially for patients with rapid neurological deficit which may require emergent surgery without biopsy, this study aimed to retrospectively review CT and magnetic resonance imaging (MRI) findings of patients with aggressive spinal GCT to describe and categorize typical and atypical features to help the imaging diagnosis.

## Materials and Methods

### Study Participants

The study design was approved by the appropriate hospital ethics committee (number IRB00006761-M2020255) and consent for the study was waived due to the de-identified retrospective review of data. Pretreatment data from 161 patients diagnosed with aggressive spinal GCTs confirmed pathologically from December 2001 to May 2020 at the participating institution was analyzed in a blind manner by an experienced radiologist, orthopedist, and pathologist.

Inclusion criteria included complete CT or MR images before treatment, showing aggressive lesion features (S3, extending to the epidural and/or paravertebral space) and pathological diagnosis of GCT. Exclusion criteria included lack of complete preoperative images, pathological diagnoses other than GCT, and GCT without aggressive features (S1 or S2). Forty-seven patients were excluded due to a lack of ideal pre-treatment imaging, and 13 patients were excluded for the final pathological diagnosis of other tumors. There were no patients with S1 or S2 lesions. Finally, 101 patients were included in our study. Clinical information for the 101 patients was collected, including age at presentation, sex, medical history, symptom duration, and neurological function.

### Imaging Procedures and Analysis

Overall, 100 patients underwent CT at the study site and 63 simultaneously underwent enhanced CT. All scans were performed with a GE Light Speed 64-slice CT scanner (General Electric, Boston, MA, USA) with a 120-kV tube voltage, 200-300-mA tube current, 3-mm slice thickness, 3-mm interval, and pitch = 1. In the enhanced scan, a non-ionic iodine-containing contrast medium was injected into the patient with a high-pressure syringe at a 3-mL/s rate and a 2-mL/kg dose.

Ninety-four patients had MRI performed at the study site and 42 patients simultaneously underwent enhanced scans. MRI was conducted using the 3-T Magnetom Trio (Siemens, Munich, Germany) and body phased-array coils with patients in the supine position. The parameters were as follows: sagittal turbo-spin echo (TSE) T1-weighted (TR [repetition time]/TE [echo time], 550 ms/11 ms), TSE T2-weighted (TR/TE, 2800 ms/109 ms), T2 reverse response sequence (TR/TE, 3440 ms/102 ms; inversion time, 200 ms), field of view (FOV) 280 · 280 mm, and axial T2-multiple echo in 2 dimensions (TR/TE, 806 ms/14 ms). Slice thicknesses and slice gaps of 3 and 0.8 mm, respectively, were utilized for all procedures. For enhanced scans, the gadolinium contrast agent gadolinium-diethylenetriaminepentaacetate (Gd-DTPA) was injected through the elbow veins at a 0.2-mmol/kg dose and 2-mL/s rate.

All these images of spinal GCT were analyzed by an experienced radiologist and an experienced surgeon in blind manner. We classify the widely accepted radiological features as typical, and features which are rarely mentioned (only case report) as atypical. Typical radiological features include osteolytic lesion, destruction of cortical bone, pathological fracture, centered in the vertebral body, epidural extension, expansile lesion, pseudotrabeulation on CT scan, low to intermediate signal intensity on the T1-weighted image, low-to-iso signal intensity or heterogeneous high-signal intensity with cystic areas on the T2-weighted image, a curvilinear area of low signal intensity on T1- and/or T2-weighted image, fluid-fluid level on T2-weighted images and marked enhancement on contrast-enhanced CT and/or MR. Atypical radiological features include involving  $\geq 2$  segments, involvement of adjacent bony structure such as the ribs, a huge paravertebral mass with relatively slight bony destruction, centered in the posterior elements, partial margin sclerosis and mineralization within the tumor on CT.

### Statistical Analyses

All collected data was analyzed with use of SPSS 23.0. Categorical variables are presented with frequencies and percentages and continuous variables as medians. Categorical variables were compared using chi-square or Fisher exact tests, and continuous variables were compared using the Student's t or Mann-Whitney U test. Significance was set a priori at  $p < 0.05$  for all analyses.

## Literature Review

A review of published radiographic studies reporting on aggressive spinal GCTs over the past 20 years was conducted using PubMed, Springer, Ovid, and EBSCO databases. Articles were included if they described a confirmed diagnosis of aggressive spinal GCTs (S3) and included CT and/or MRI images. All typical and atypical features were grouped according to the diagnostic standards used in the present study.

## Results

### Patients

All 101 patients (44 males and 57 females, 1:1.3 ratio) had S3 lesions, and no patients with S1 or S2 lesions were found in the study-site database. The average age at diagnosis was 32.5 years (range, 7-71 years) and most incidences occurred when patients were in their 30s ( $n = 38$ ) and 40s ( $n = 23$ ). All patients had confirmed pathological diagnosis based on CT-guided percutaneous biopsies and/or open surgical procedure.

### Clinical Data

The average time between the presentation of symptoms and clinical diagnosis was 5.9 months (range, 0.6-24 months). Local pain was the most common symptom, experienced by 86.1% (87/101) of the patients. In addition, 79.2% (80/101) of the patients experienced neurological deficits including radiculopathy (58.4%, 59 patients), myelopathy (40.6%, 41 patients) and/or cauda equina syndrome (7.9%, 8 patients).

### Radiographic Findings

**Location.** Among 101 patients, 99 had only one lesion and 2 had lung metastases. In total, 36, 40, 23, and 2 lesions originated in the cervical spine, thoracic spine, lumbar spine, and cervicothoracic junction, respectively. Ninety lesions (89.1%) occurred in the vertebral body, of which 82 extended to the neural arch (Figure 1), while 11 lesions (10.9%) were centered in the posterior elements and all of these extended to the vertebral body (Figure 2).

At diagnosis, 82 lesions (81.2%) involved only 1 segment, 11 lesions (10.9%) involved 2 adjacent segments, and 8 lesions (7.9%) involved 3 adjacent segments (Figure 3). Seven lesions involved adjacent ribs (Figure 3D). Among 19 lesions involving over 1 segment, one extended into the ventral part of the cranial and caudal vertebral body, indicating that the tumor might extend through the anterior longitudinal ligament (Figure 4A, B); 4 lesions involved the dorsal part of the adjacent vertebral bodies, indicating that the tumor might extend through the posterior longitudinal ligament (Figure 4C); 2 lesions involved multiple adjacent articular facets, indicating that the tumor might extend through the ligament of the facet joint (Figure 4D, E).

All patients had S3 lesions, 6 lesions extended into the paravertebral area, 5 lesions to the spinal canal, and 90 lesions to

both the paravertebral area and spinal canal. Forty-eight lesions (47.5%) compressed the spinal cord (Figure 5). Ten lesions had a huge paravertebral mass extending over 2 segments with slight bone destruction and were classified as paravertebral type (Figure 6). These lesions were located on the edge of the thoracic vertebrae and expanded into the thoracic cavity except 1 located in the cervical vertebrae. In these 10 lesions, the average symptom duration was 3.7 months and 4 patients had neurological deficits, of which 1 had radiculopathy and 3 had myelopathy, including Frankel grade C (1), D (2), and E (1).

**CT findings.** In total, 100 patients had CT scans and all lesions were osteolytic with cortical destruction (discontinuous or incomplete). Overall, 82 lesions showed collapse of the vertebral body and/or pathological fracture (Figure 1), 78 lesions had pseudotrabeulation (Figure 5A), and 74 lesions were expansile. Partial margin sclerosis was observed in 16 lesions (Figure 7) and mineralization within the tumor was observed in 3 lesions, manifested as striped high-density shadows in the rim of the paravertebral mass on CT scans (Figure 6).

**MRI findings.** In total, 94 patients had MRI, and all lesions had low to intermediate signal intensity on the T1-weighted image, including 10 lesions (10.6%) contained small high-signal-intensity areas, suggesting recent hemorrhage (Figure 8). Fifty-eight lesions (61.7%) show a curvilinear area of low signal intensity on T1- and/or T2-weighted images, which may correspond to bony septa or hemosiderin deposit on CT (Figure 8). On T2-weighted images, we divided the signal into 4 types: (a) significantly low signal intensity (6 lesions, 6.4%); (b) low-to-iso signal intensity with or without cystic high-signal areas (48 lesions, 51.1%); (c) heterogeneous high-signal intensity with many cystic areas (32 lesions, 34.0%); (d) homogeneous high-signal intensity (8 lesions, 8.5%) (Figure 9). Furthermore, 9 lesions (9.57%) showed a fluid–fluid level on T2-weighted images (Figure 2B).

**Enhancing pattern.** In total, 72 patients underwent contrast-enhanced CT and/or MR scan and showed marked (61, 84.7%), moderate (8, 11.1%), and mild (2, 2.8%) enhancement, and 1 case (1.1%) was unenhanced.

**Typical and atypical radiographic features.** Typical radiological features included: (1) osteolytic lesion ( $n = 101$  100%); (2) destruction of cortical bone, manifested as discontinuous or incomplete ( $n = 101$  100%); (3) collapse of the vertebral body and/or pathological fracture ( $n = 82$ , 82.0%); (4) lesions centered in the vertebral body ( $n = 90$ , 89.1%); (5) epidural extension ( $n = 95$ , 94.1%), and compressing the spinal cord ( $n = 48$ , 47.5%); (6) expansile lesion ( $n = 74$ , 73.3%); (7) pseudotrabeulation on CT scan ( $n = 78$ , 78.0%); (8) low to intermediate signal intensity on the T1-weighted image ( $n = 94$  100%); (9) low-to-iso signal intensity or heterogeneous high-signal intensity with cystic areas on the T2-weighted image ( $n = 80$ , 85.1%); (10) a curvilinear area of low signal intensity on T1- and/or T2-weighted image ( $n = 58$ , 61.7%); (11) fluid–fluid level on T2-weighted images ( $n = 9$ , 9.57%); (12) marked

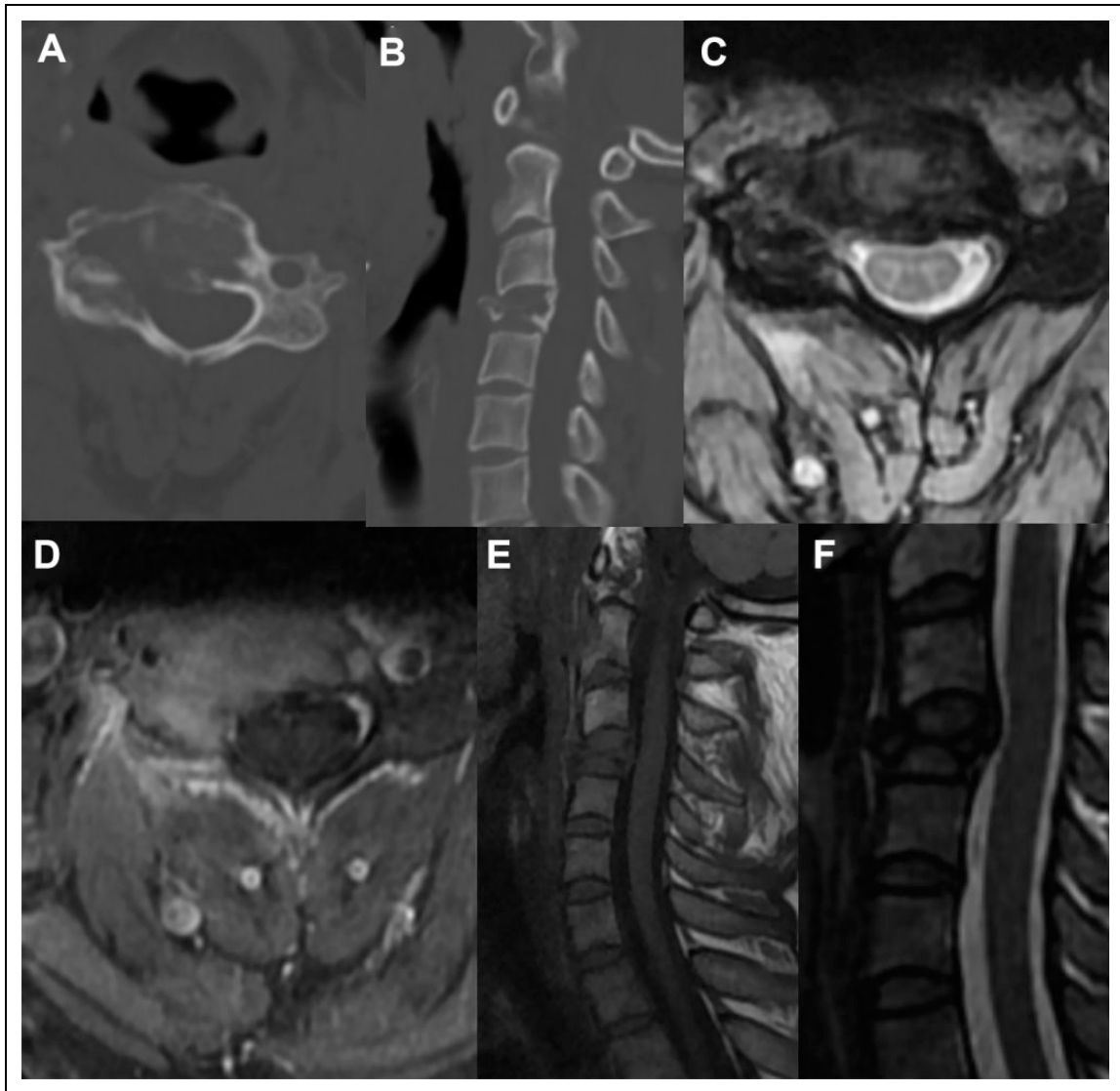


**Figure 1.** Imaging from a 32-year-old man with a typical aggressive giant cell tumor at C4. The patient had local pain in the neck and right shoulder for 12 months (Frankel E). A, Axial CT scan shows an expansile, osteolytic lesion centered in the vertebral body of C4, extending to the right pedicle of the vertebral arch. The cortical bone is also destroyed. B, A sagittal CT scan shows the pathological fracture and collapse of the vertebral body. C, Axial T2-weighted MRI shows the epidural extension. D, Contrast-enhanced MRI shows the marked enhancement. E and F, Sagittal T1-weighted and T2-weighted MRI show intermediate and hypointense signals, respectively.

enhancement on contrast-enhanced CT and/or MR ( $n = 61$ , 84.7%).

Atypical features included: (1) GCT involving  $\geq 2$  segments ( $n = 19$ , 18.8%), involvement of adjacent bony structure ( $n = 7$ , 6.9%); (2) paravertebral subtype defined by a huge paravertebral mass with relatively slight bony destruction ( $n = 10$ , 9.9%); (3) lesions centered in the posterior elements ( $n = 11$ , 10.9%); (4) partial margin sclerosis on the CT scan ( $n = 16$ , 16.0%); (5) mineralization within the tumor on CT ( $n = 3$ , 3.0%).

Lesions in 41 patients (40.6%) had at least 1 atypical radiographic feature, of these, 28 had only 1 atypical feature, 9 had 2 atypical features, 3 had 3 atypical features, and 1 had 4 atypical features.

Differences in age, sex, symptom duration, lesion location, and Frankel grade between patients with aggressive GCTs with and without atypical radiographic features are summarized in Table 1. Lesion distribution was the only significantly different radiographic feature between groups ( $p = 0.016$ ). Patients in the atypical group were older and had a longer time between symptom presentation and diagnosis, but these differences were not significant.

#### *Percutaneous CT-Guided Biopsy*

Thirteen patients underwent emergent surgery without preoperative pathology due to dyspnea and/or severe spinal cord injury. Eighty-eight patients (87.1%) underwent percutaneous



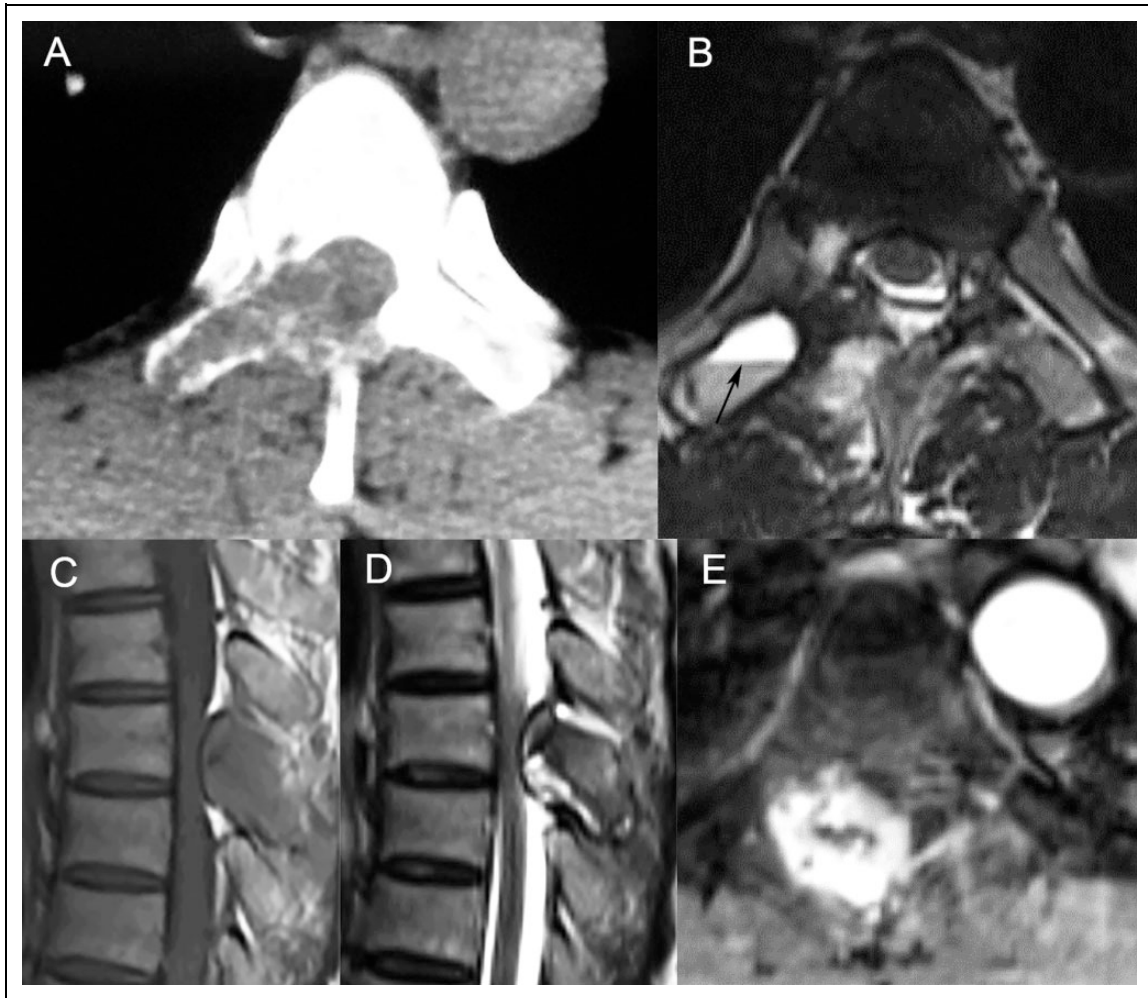


**Figure 2.** Imaging from a 37-year-old man who experienced severe back pain for 2 months. A, Axial CT scan shows an expansile osteolytic lesion centered in the pedicle of T5 and extending to the spinal canal. B, Axial T2-weighted MRI showed the presence of the fluid–fluid level (black arrow). C, Sagittal T1-weighted MRI shows low-to-intermediate signal intensity. D, Sagittal T2-weighted MRI shows intermediate signal intensity. E, Axial MRI shows marked enhancement after the administration of gadolinium.

CT-guided biopsy, including 37 patients with atypical features and 51 patients without atypical features, and 83 patients (94.3%) were pathologically confirmed with GCTs. In the atypical group, 3 patients (8.1%) were misdiagnosed with a brown tumor, aneurysmal bone cyst, and GCT of the tendon sheath. In the typical group, 2 patients (3.9%) were misdiagnosed with osteoblastoma and aneurysmal bone cyst.

### Literature Review

We reviewed studies on aggressive GCT published over the past 20 years according to PRISMA statement, and 52 studies were involved (Figure 10).<sup>15-66</sup> There were 60 patients with 53 CT scans and 39 MRI scans, of whom 21 patients underwent enhanced scans simultaneously. The typical and atypical features were summarized according to the diagnostic standards in the present study (Table 2) and the frequency of the features was similar. Lesions in 24 patients (40.0%) had at least 1

atypical radiographic feature, of which 16 had only 1 atypical feature, 6 had 2 atypical features, and 2 had 3 atypical features.

### Discussion

In this study, we analyzed radiographic data from 101 patients with aggressive GCT of the mobile spine and classified the features as typical or atypical. The results indicate that about 40% of the GCTs exhibit at least one atypical feature. The results add to existing knowledge on the incidence and types of radiological features associated with spinal GCTs and are consistent with previous literature.<sup>4,13,14,67</sup> In this series, spinal GCTs are more likely to occur in patients aged between 20 and 40 years and have a slightly higher incidence in women, the average time between symptomatic presentation and clinical diagnosis is 5.9 months, and local pain is the most common symptom. Furthermore, 2% (2/101) of patients had pulmonary metastasis, which was reported to occur in 2-3% of patients with GCTs at diagnosis.<sup>67,68</sup> We briefly reviewed data on

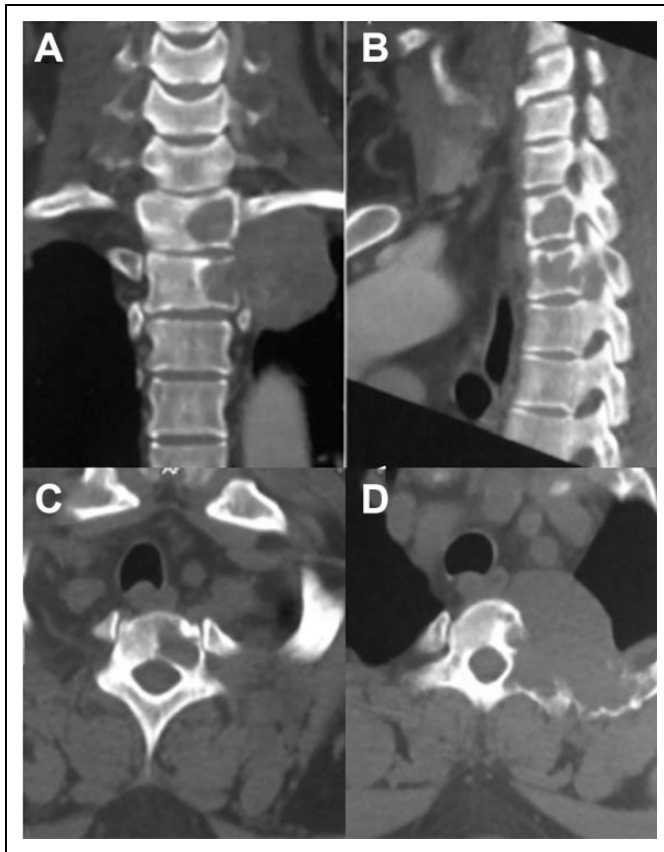


**Figure 3.** Imaging from a 37-year-old man who experienced local pain in the neck, upper back, and left shoulder for 4 months. A, Coronal CT scan shows an expansile, osteolytic lesion with a huge mass lesion formation in the paravertebral area at T1 and T2, belonging to the paravertebral type. B, Sagittal CT scan shows the destruction of the cortical bone and the pathological fracture of T2. C and D, Axial CT scan shows the involvement of the vertebral body of T1, T2, and the second rib.

aggressive spinal GCT, and the frequency of typical and atypical features was similar to that observed in our study. To our knowledge, this is the largest analysis of the imaging features of aggressive GCT of the spine, especially for the atypical imaging features which are only mentioned in several case reports.

The paravertebral type of GCT, manifesting as a huge paravertebral mass extending over 2 segments with slight bone destruction, has only been presented in a few case reports.<sup>30</sup> These lesions are usually located on the edge of thoracic vertebrae, expand into the thoracic cavity, and are associated with slight neurological deficits. Its radiological features might lead to misdiagnosis as a malignant tumor. In the present study, the 10 patients with paravertebral type had an average symptom duration of 3.7 months and 4 patients had slight neurological deficits, including one Frankel grade C. This may be because the lesions develop slowly over a long period. Intralesional bleeding might make the lesions symptomatic, leading to diagnosis.

GCT in the extremities rarely extends to the adjacent bone, while in this study, the lesions extended to adjacent vertebrae in 19 patients and adjacent ribs in 7 patients. Tomita et al. suggested that metastatic tumors might extend to adjacent vertebrae through anterior and/or posterior longitudinal ligaments. It seems that the GCTs extend through other ligaments such as the capsule of articular facets and the costotransverse joint (Figure 4).

GCTs in the extremities are usually eccentric, while this is not typical in the spine. Spinal GCT is usually located in the vertebral body, accounting for approximately 85-100% of cases according to the literature.<sup>6,15,17</sup> In our series, lesions arose from the vertebral body in 90 patients and the posterior neural arch in 11 patients. GCT lesions centered in the posterior elements should be differentially diagnosed from

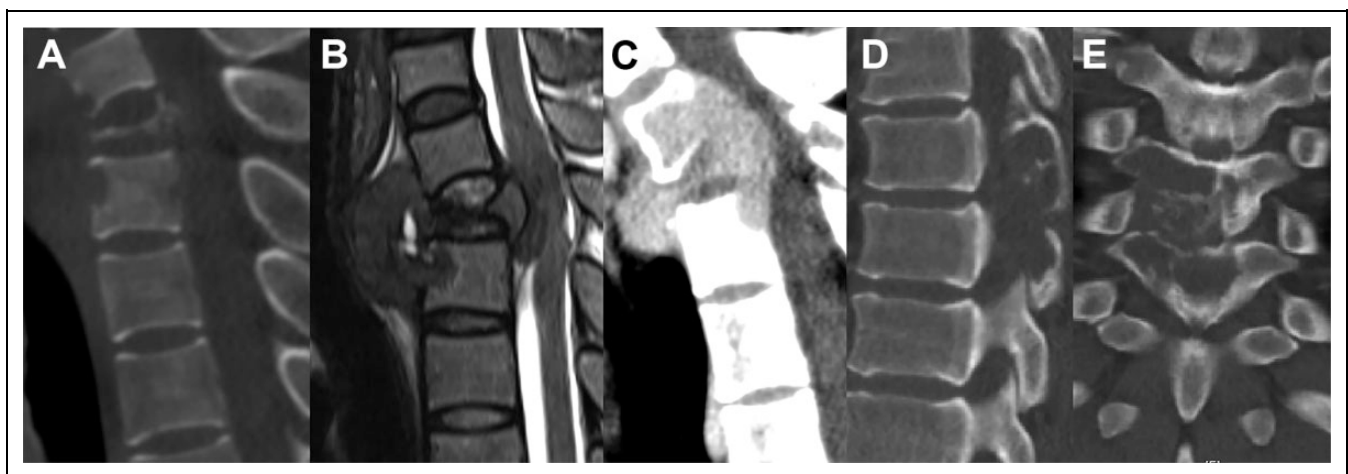


**Figure 4.** A and B, A giant cell tumor of C7-T2 in a 35-year-old woman, sagittal CT scan (A) shows a compression fracture of T1. Sagittal T2-weighted MRI (B) shows involvement of the ventral part of multiple adjacent vertebral bodies, indicating the tumor might extend through the anterior longitudinal ligament. C, A giant cell tumor of C7-T2 in a 36-year-old woman. The sagittal CT scan shows involvement of the dorsal part of the multiple adjacent vertebral bodies, indicating the tumor extended through the posterior longitudinal ligament. D and E, A giant cell tumor of T7-T8 in a 46-year-old man, sagittal and coronal CT scans show the involvement of the adjacent facet joint, indicating the tumor might extend through the interspinous ligament or the ligament of the facet joint.

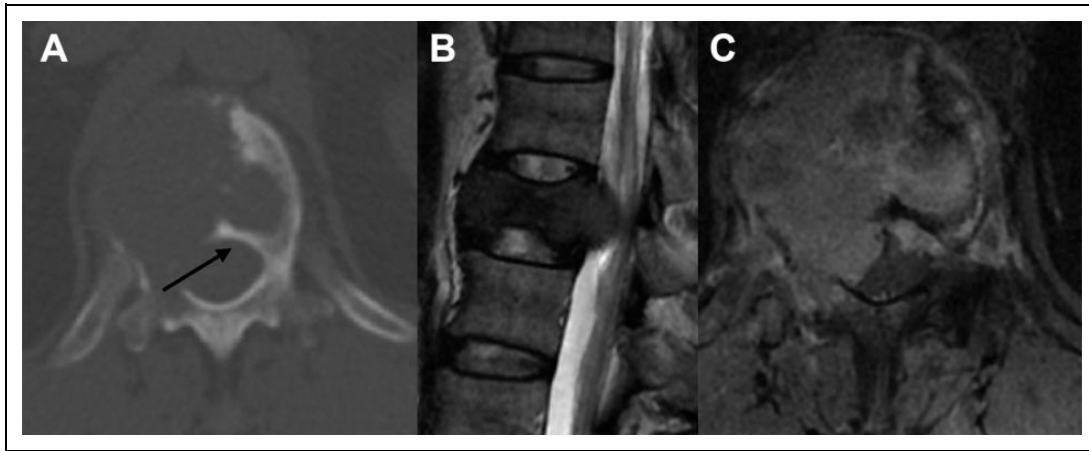


**Figure 5.** Imaging from a 42-year-old woman who experienced myelopathy for 8 months (Frankel grade D). A, Axial CT scan shows an aggressive GCT lesion at T12 with long bony septa (black arrow). B, Sagittal T2-weighted MRI shows a low signal intensity and the spinal cord is compressed. C, Contrast-enhanced axial T1-weighted MR image shows moderate enhancement and the lesion extends to the spinal canal with compression of the spinal cord.

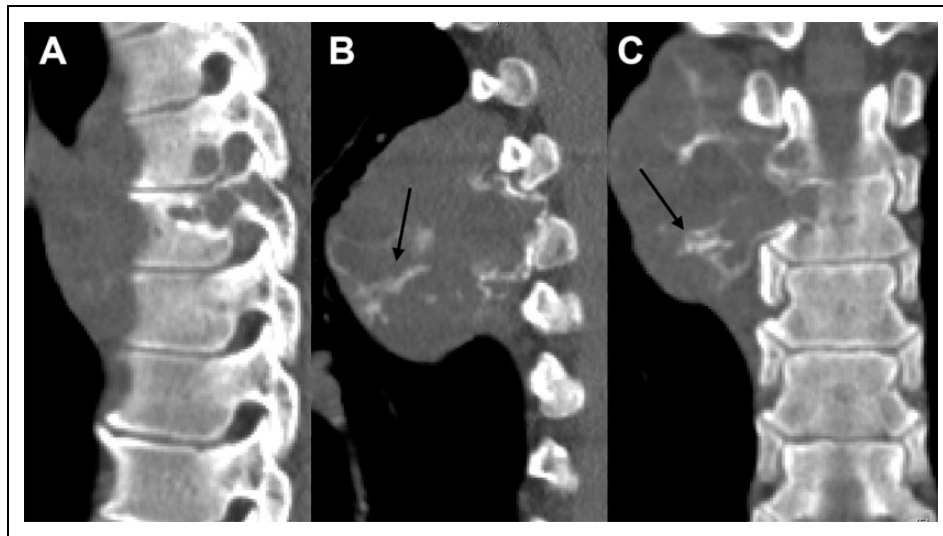


**Figure 6.** Imaging from a 40-year-old woman who experienced severe back pain for 3 months. A, Sagittal CT scan shows osteolytic lesions at T4 and T5. B and C, Sagittal and coronal CT scans show a huge mass lesion formation in the paravertebral area, and mineralization is seen in the rim of the paravertebral mass (black arrows).

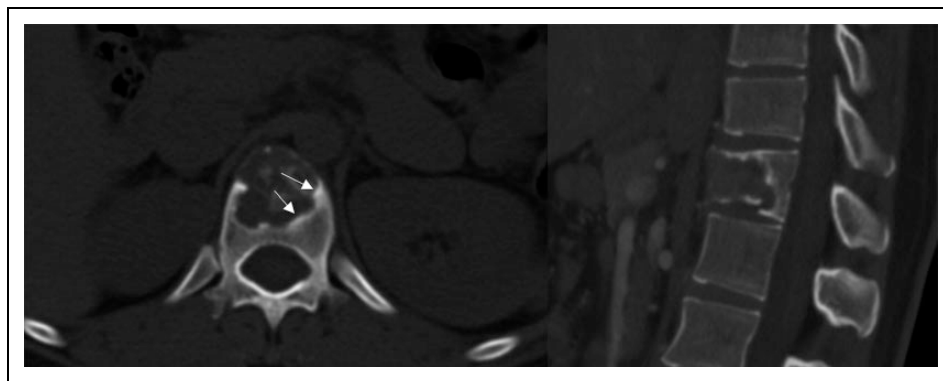


**Figure 7.** Imaging from a 27-year-old woman who experienced severe pain of low back for 8 months. Axial and sagittal CT scans show an osteolytic lesion with a partly sclerotic margin (white arrows) at T12.



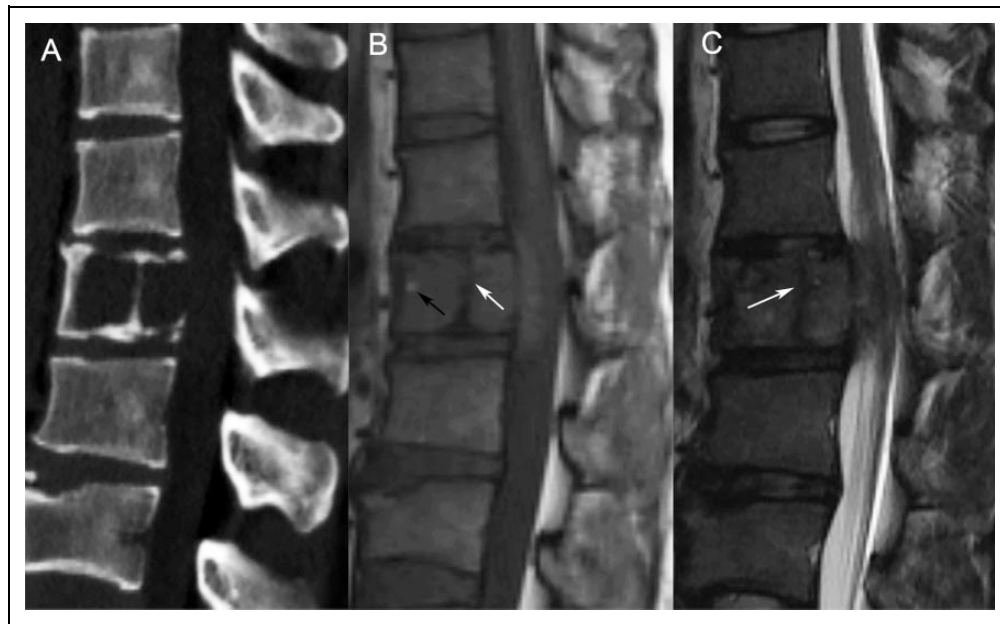


**Figure 8.** Imaging from a 26-year-old man who experienced low back pain with radiating pain to the left lower extremity for 6 months (Frankel D). Sagittal CT scan (A) shows an aggressive GCT lesion at L1 with long bony septa. Sagittal T1-weighted (B) and T2-weighted (C) MRI show a curvilinear low signal area (white arrows) within the mass, corresponding to bony septa on CT. There is a small high-signal-intensity area on T1-weighted MRI (black arrow), suggesting a relatively recent hemorrhage.

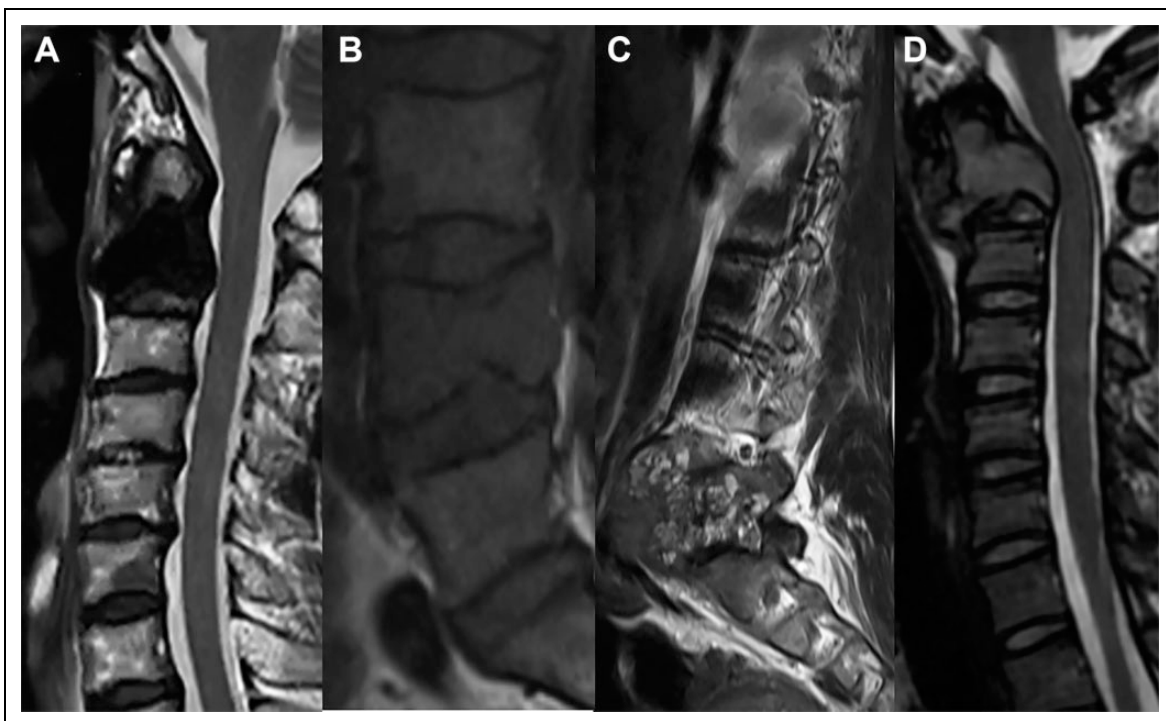


**Figure 9.** A, Giant cell tumor of C2 in a 55-year-old woman with the T2-weighted MRI showing significantly low signal intensity. B, Giant cell tumor of L4 in a 39-year-old man with the T2-weighted MRI showing homogeneous low to intermediate signal intensity. C, Giant cell tumor of L5 in a 23-year-old woman with the T2-weighted MRI showing heterogeneous high-signal intensity with multiple cystic changes. D, Giant cell tumor of C2 in a 16-year-old woman, T2-weighted MRI shows homogeneous high-signal intensity.



**Table 1.** Comparison of Patient Characteristics in the Typical and Atypical Groups.

Factors	Typical Group (N = 60)	Atypical Group (N = 41)	T, Z, or Chi-Square Value	P Value
Age* (y)	31.2 ± 14.0	34.5 ± 11.4	-1.230	0.222
Sex (female/male)	35/25	22/19	0.216	0.642
Symptom duration† (month)	3.0 (4.0)	4.0 (7.0)	-1.194	0.233
Main lesion location			9.217	0.016
Cervical	26	10		
Thoracic	18	22		
Lumbar	16	7		
Crossed the cervico-thoracic junction	0	2		
Frankel grade			2.706	0.445
B	1	0		
C	6	1		
D	19	14		
E	34	26		

\*The values are given as the mean and the standard deviation. †The values are given as the median, with the interquartile range in parentheses.

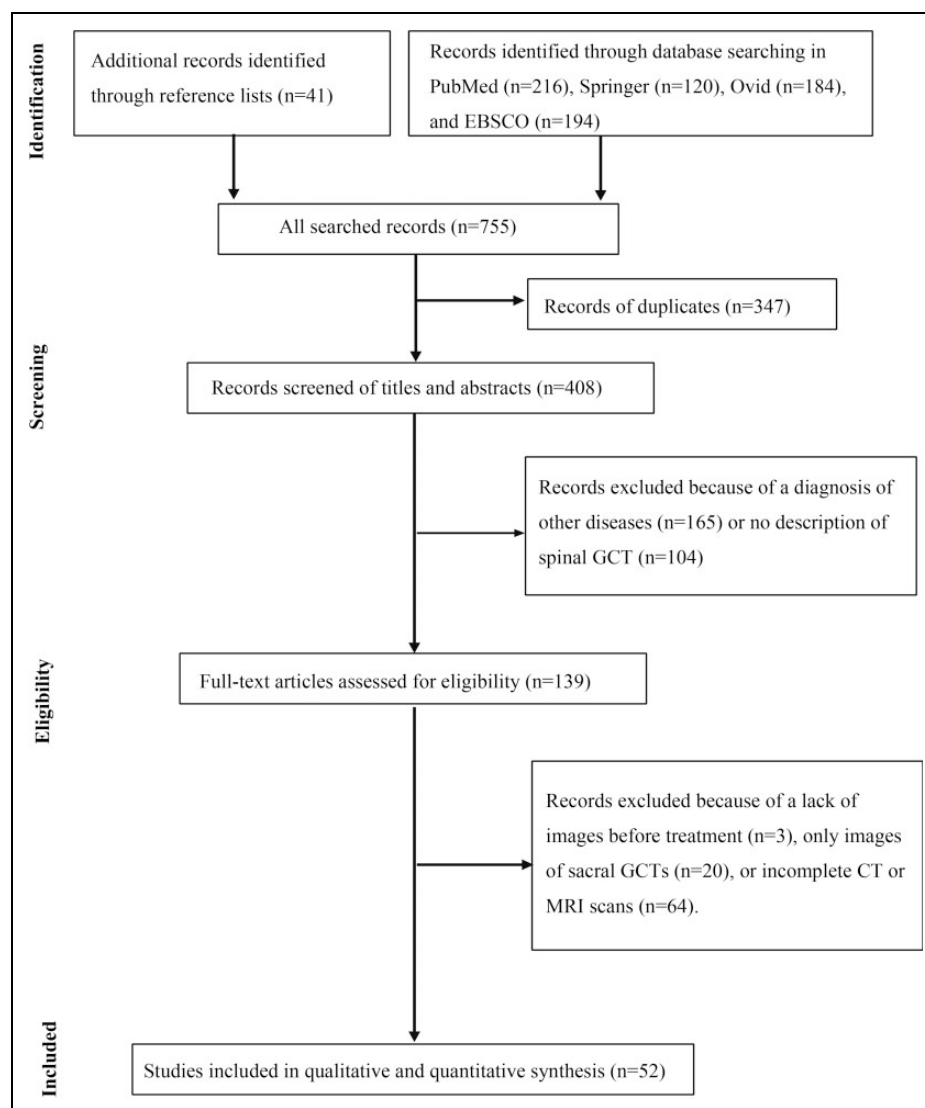


**Figure 10.** Flow of information through the different phases of literature review. CT, computed tomography; GCT, giant cell tumor; MRI, magnetic resonance imaging.

**Table 2.** Summary of Typical and Atypical Features Observed in a Review of the Literature.<sup>a</sup>

Typical features	No. (%) of cases	Atypical features	No. (%) of cases
Osteolytic lesion	60 (100%)	Involving $\geq 2$ segment	10 (16.7%)
Expansile lesion	47 (78.3%)	Paravertebral type	7 (11.7%)
Destruction of cortical bone	53 (100%)	Lesions centered in the posterior elements	8 (13.3%)
Collapse of the vertebral body	38 (71.7%)	Partial margin sclerosis on CT scan	8 (15.1%)
Centered in the vertebral body	52 (86.7%)	Mineralization within the tumor	1 (1.9%)
Epidural extension	56 (93.3%)		
Compressing the spinal cord	29 (48.3%)		
Pseudotrabeclulation on CT	40 (75.5%)		
Low to intermediate signal intensity on the T1-weighted image	38 (97.4%)		
Low-to-iso signal intensity or heterogeneous High-signal intensity with cystic areas on the T2-weighted image	33 (84.6%)		
Fluid–fluid level on T2-weighted images	4 (10.3%)		
A curvilinear area of low signal intensity on MRI	22 (56.4%)		
Marked enhancement on contrast-enhanced CT and/or MR	16 (76.2%)		

<sup>a</sup> CT and/or MRI reviewed for 60 patients from 52 studies published in the past 20 years.

osteoblastoma, a primary aneurysmal bone cyst, and GCT of the tendon sheath.

Although GCT is generally recognized as having a non-sclerotic margin,<sup>4</sup> areas of peripheral sclerosis have been reported in up to 33% of cases.<sup>15,69</sup> In the present study, partial margin sclerosis was observed on the CT scan in 16.0% of lesions. This manifestation may be related to the relatively slow tumor growth.

There should be no matrix mineralization within GCTs according to the literature,<sup>70</sup> but striped high-density shadows were observed in the rim of the paravertebral mass on CT scans in 3 cases in this study. Further pathological analysis showed ossification and calcification, reflecting the repair response after bone destruction and calcium deposition on the periphery of the tumor, which is an atypical radiological feature for the diagnosis of spinal GCT.

Besides image findings, the diagnosis of GCTs relies on CT-guided biopsy. The reported accuracies of CT-guided biopsy of the musculoskeletal system and spine are 94% and 89%, respectively.<sup>11</sup> In this study, 88 patients underwent CT-guided biopsy with an accuracy rate of 94.3%. In total, 12.9% of patients required emergency surgery without preoperative biopsy, so the radiologic features played an important role in the preoperative clinical diagnosis of aggressive spinal GCT.

In the study-site database, all lesions were classified as Enneking stage 3, but S2 lesions reportedly account for 75% of GCTs in the extremities and about 20% of spine GCTs.<sup>6,67</sup> This result may be because most patients in China do not have radiological examinations until they have obvious symptoms and tumors are not often diagnosed in the early stage. Moreover, patients with S1 and S2 lesions may be treated in local hospitals, and not referred to the study site, which is a tertiary spine center.

This study had several limitations to consider. First, this was a retrospective analysis of results over 20-years from a single center. Future multi-center prospective research is needed. Second, there were 101 cases, which is a small sample for robust statistical analysis and more cases are needed to strengthen the results. Finally, further pathological studies are recommended to analyze the causes of atypical features.

In conclusion, about 40% of the aggressive GCT lesions had at least 1 atypical feature. CT-guided biopsies are recommended for pathological diagnosis.

### Authors' Note

Bei Yuan, MD, Lihua Zhang, MD, and Shaomin Yang, MD, contributed equally to this work.


### Declaration of Conflicting Interests

The author(s) declared no potential conflicts of interest with respect to the research, authorship, and/or publication of this article.

### Funding

The author(s) disclosed receipt of the following financial support for the research, authorship, and/or publication of this article: This work was supported by Peking University Third Hospital [Y71508-01]; and Capital's Funds for Health Improvement and Research [2020-4-40916].

### ORCID iD

Bei Yuan, MD  <https://orcid.org/0000-0003-4050-9605>

### References

1. Amanatullah DF, Clark TR, Lopez MJ, Borys D, Tamurian RM. Giant cell tumor of bone. *Orthopedics*. 2014;37(2):112-120. doi: 10.3928/01477447-20140124-08

2. Sung HW, Kuo DP, Shu WP, Chai YB, Liu CC, Li SM. Giant-cell tumor of bone: analysis of two hundred and eight cases in Chinese patients. *J Bone Joint Surg Am.* 1982;64(5):755-761.
3. Mendenhall WM, Zlotecki RA, Scarborough MT, Gibbs CP, Mendenhall NP. Giant cell tumor of bone. *Am J Clin Oncol.* 2006;29(1):96-99. doi:10.1097/01.coc.0000195089.11620.b7
4. Turcotte RE. Giant cell tumor of bone. *Orthop Clin North Am.* 2006;37(1):35-51. doi:10.1016/j.ocl.2005.08.005
5. Wu JS, Hochman MG. Bone tumors. A practical guide to imaging. *Anticancer Res.* 2012;32(12):5538.
6. Boriani S, Bandiera S, Casadei R, et al. Giant cell tumor of the mobile spine: a review of 49 cases. *Spine (Phila Pa 1976).* 2012; 37(1):E37-E45. doi:10.1097/BRS.0b013e3182233ccd
7. Enneking WF. A system of staging musculoskeletal neoplasms. *Clin Orthop Relat Res.* 1986;(204):9-24.
8. Bidwell JK, Young JW, Khalluff E. Giant cell tumor of the spine: computed tomography appearance and review of the literature. *J Comput Tomogr.* 1987;11(3):307-311.
9. Hau A, Kim I, Kattapuram S, et al. Accuracy of CT-guided biopsies in 359 patients with musculoskeletal lesions. *Skeletal Radiol.* 2002;31(6):349-353.
10. Rimondi E, Staals EL, Errani C, et al. Percutaneous CT-guided biopsy of the spine: results of 430 biopsies. *Eur Spine J.* 2008; 17(7):975-981. doi:10.1007/s00586-008-0678-x
11. Rimondi E, Rossi G, Bartalena T, et al. Percutaneous CT-guided biopsy of the musculoskeletal system: results of 2027 cases. *Eur J Radiol.* 2011;77(1):34-42. doi:10.1016/j.ejrad.2010.06.055
12. Chakarun CJ, Forrester DM, Gottsegen CJ, Patel DB, White EA, Matcuk GR. Giant cell tumor of bone: review, mimics, and new developments in treatment. *Radiographics.* 2013;33(1):197-211. doi:10.1148/rg.331125089
13. Junming M, Cheng Y, Dong C, et al. Giant cell tumor of the cervical spine: a series of 22 cases and outcomes. *Spine.* 2008; 33(3):280-288. doi:10.1097/BRS.0b013e318162454f
14. Martin C, McCarthy EF. Giant cell tumor of the sacrum and spine: series of 23 cases and a review of the literature. *Iowa Orthop J.* 2010;30:69-75.
15. Shi LS, Li YQ, Wu WJ, Zhang ZK, Gao F, Latif M. Imaging appearance of giant cell tumour of the spine above the sacrum. *Br J Radiol.* 2015;88(1051):20140566. doi:10.1259/bjr.20140566
16. Kwon JW, Chung HW, Cho EY, et al. MRI findings of giant cell tumors of the spine. *AJR Am J Roentgenol.* 2007;189(1):246-250. doi:10.2214/AJR.06.1472
17. Si MJ, Wang CG, Wang CS, et al. Giant cell tumours of the mobile spine: characteristic imaging features and differential diagnosis. *Radiol Med.* 2014;119(9):681-693. doi:10.1007/s11547-013-0352-1
18. Xara-Leite F, Coutinho L, Fleming C, et al. Can denosumab cure giant cell tumors of the spine? A case report and literature review. *Eur J Orthop Surg Traumatol.* 2020;30(1):19-23. doi:10.1007/s00590-019-02554-9
19. Sertbas I, Karatay M, Hacisalihoglu UP. Cervical spine giant cell bone tumor: a case report. *World J Surg Oncol.* 2019;17(1):82. doi:10.1186/s12957-019-1625-5
20. Yoshioka K, Kawahara N, Murakami H, et al. Cervicothoracic giant cell tumor expanding into the superior mediastinum: total excision by combined anterior-posterior approach. *Orthopedics.* 2009;32(7):531. doi:10.3928/01477447-20090527-26
21. Osaka S, Sugita H, Osaka E, et al. Clinical and immunohistochemical characteristics of benign giant cell tumour of bone with pulmonary metastases: case series. *J Orthop Surg (Hong Kong).* 2004;12(1):55-62.
22. Jia Q, Chen G, Cao J, et al. Clinical features and prognostic factors of pediatric spine giant cell tumors: report of 31 clinical cases in a single center. *Spine J.* 2019;19(7):1232-1241. doi:10.1016/j.spinee.2019.02.011
23. Liu S, Zhou X, Song A, Huo Z, Wang Y, Liu Y. Combining two-stage surgery and denosumab treatment in a patient with giant cell tumour of the lumbar spine with intraperitoneal growth. *Postgrad Med J.* 2019;95(1120):106-107. doi:10.1136/postgradmedj-2018-135972
24. Ando K, Kobayashi K, Machino M, et al. Computed tomography-based navigation system-assisted surgery for primary spine tumor. *J Clin Neurosci.* 2019;63:22-26. doi:10.1016/j.jocn.2019.02.015
25. Kajiwaru D, Kamoda H, Yonemoto T, et al. Denosumab for treatment of a recurrent cervical giant-cell tumor. *Asian Spine J.* 2016; 10(3):553-557. doi:10.4184/asj.2016.10.3.553
26. Boriani S, Cecchinato R, Cuzzocrea F, Bandiera S, Gambarotti M, Gasbarrini A. Denosumab in the treatment of giant cell tumor of the spine. Preliminary report, review of the literature and protocol proposal. *Eur Spine J.* 2020;29(2):257-271. doi:10.1007/s00586-019-05997-0
27. Singh P, Chaudhry M, Singh A. Emergency diagnosis of giant cell tumour (GCT) of spine by image guided fine needle aspiration cytology (FNAC). *J Clin Diagn Res.* 2014;8(7):FD07-8. doi:10.7860/JCDR/2014/8845.4564
28. Afsoun S, Saied SA, Amir N, Hamed J. En-bloc resection of a giant cell tumor causing cervical vertebral collapse. *Asian J Neurosurg.* 2018;13(1):150-153. doi:10.4103/1793-5482.181136
29. Kathiresan AS, Johnson JN, Hood BJ, Montoya SP, Vanni S, Gonzalez-Quintero VH. Giant cell bone tumor of the thoracic spine presenting in late pregnancy. *Obstet Gynecol.* 2011;118(2 Pt 2): 428-431. doi:10.1097/AOG.0b013e31821081a2
30. Demura S, Kawahara N, Murakami H, et al. Giant cell tumor expanded into the thoracic cavity with spinal involvement. *Orthopedics.* 2012;35(3):e453-e456. doi:10.3928/01477447-20120222-42
31. Metkar U, Wardak Z, Katz DA, Lavelle WF. Giant cell tumor of a lumbar vertebra in a 7-year-old child: a case report. *J Pediatr Orthop.* 2012;32(8):e76-e80. doi:10.1097/BPO.0b013e31826193e7
32. Michalowski MB, Pagnier-Clémence A, Chirossel JP, et al. Giant cell tumor of cervical spine in an adolescent. *Med Pediatr Oncol.* 2003;41(1):58-62.
33. Mahajan R, Chhabra HS, Tandon V, Venkatesh R. Giant cell tumor of cervicothoracic region treated by triple corpectomy from posterior only approach: a case report with review of literature. *J Craniovertebr Junction Spine.* 2015;6(4):212-215. doi:10.4103/0974-8237.167885

34. Shimada Y, Hongo M, Miyakoshi N, et al. Giant cell tumor of fifth lumbar vertebrae: two case reports and review of the literature. *Spine J*. 2007;7(4):499-505. doi:10.1016/j.spinee.2006.01.016
35. Cebula H, Boujan F, Beaujeux R, Boyer P, Froelich S. Giant cell tumor of the C2 colonized by an aneurismal bone cyst. Report of case [in French]. *Neurochirurgie*. 2012;58(6):376-381. Tumeur a cellules geantes de C2 colonisee par un kyste aneurismal. A propos d'un cas. doi:10.1016/j.neuchi.2012.03.008
36. Samartzis D, Foster WC, Padgett D, Shen FH. Giant cell tumor of the lumbar spine: operative management via spondylectomy and short-segment, 3-column reconstruction with pedicle recreation. *Surg Neurol*. 2008;69(2):138-141; discussion 141-2. doi:10.1016/j.surneu.2007.01.038
37. Zabalo G, Ortega R, Vazquez A, Carballares I, Diaz J, Portillo E. Giant cell tumor of the lumbar spine. Case report and review of the literature [in Spanish]. *Neurocirugia (Astur)*. 2015;26(5):251-255. Tumor de celulas gigantes de raquis lumbar. Caso clinico y revision de la literatura. doi:10.1016/j.neucir.2014.11.008
38. Zheng K, Xu M, Wang B, Yu XC, Hu YC. Giant cell tumor of the mobile spine occurring in pregnancy: a case report and literature review. *Orthop Surg*. 2017;9(2):252-256. doi:10.1111/os.12333
39. Shirzadi A, Drazin D, Bannykh S, Danielpour M. Giant cell tumor of the odontoid in an adolescent male: radiation, chemotherapy, and resection for recurrence with 10-year follow-up. *J Neurosurg Pediatr*. 2011;8(4):367-371. doi:10.3171/2011.7.PEDS10566
40. Ben Nsir A, Said IB, Badri M, Boughamora M, Jemel H. Giant cell tumor of the sixth thoracic vertebra: case report. *Turk Neurosurg*. 2015;25(3):475-478. doi:10.5137/1019-5149.JTN.8361-13.0
41. Maldonado-Romero LV, Sifuentes-Giraldo WA, Martínez-Rodrigo MA, de la Puente-Bujidos C. Giant cell tumor of the spine: a rare cause of cervical pain. *Reumatología Clínica (English Edition)*. 2017;13(1):58-59. doi:10.1016/j.reumae.2016.03.005
42. Yonezawa N, Murakami H, Kato S, Takeuchi A, Tsuchiya H. Giant cell tumor of the thoracic spine completely removed by total spondylectomy after neoadjuvant denosumab therapy. *Eur Spine J*. 2017;26(Suppl 1):236-242. doi:10.1007/s00586-017-5086-7
43. Erdogan B, Aydin MV, Sen O, Sener L, Bal N, Yalcin O. Giant cell tumour of the sixth cervical vertebrae with close relationship to the vertebral artery. *J Clin Neurosci*. 2005;12(1):83-85. doi:10.1016/j.jocn.2004.02.017
44. Mestiri M, Bouabdellah M, Bouzidi R, et al. Giant cells tumor recurrence at the third lumbar vertebra. *Orthop Traumatol Surg Res*. 2010;96(8):905-909. doi:10.1016/j.otsr.2010.05.009
45. Hunter CL, Pacione D, Hornyak M, Murali R. Giant-cell tumors of the cervical spine: case report. *Neurosurgery*. 2006;59(5):E1142-E1143; discussion E1143. doi:10.1227/01.NEU.0000245589.08463.8D
46. Smitherman SM, Tatsui CE, Rao G, Walsh G, Rhines LD. Image-guided multilevel vertebral osteotomies for en bloc resection of giant cell tumor of the thoracic spine: case report and description of operative technique. *Eur Spine J*. 2010;19(6):1021-1028. doi:10.1007/s00586-009-1273-5
47. Santiago-Dieppa DR, Hwang LS, Bydon A, Gokaslan ZL, McCarthy EF, Witham TF. L4 and L5 spondylectomy for en bloc resection of giant cell tumor and review of the literature. *Evid Based Spine Care J*. 2014;5(2):151-157. doi:10.1055/s-0034-1387804
48. Hu Y, Xia Q, Ji J, Miao J. One-stage combined posterior and anterior approaches for excising thoracolumbar and lumbar tumors: surgical and oncological outcomes. *Spine*. 2010;35(5):590-595. doi:10.1097/BRS.0b013e3181b967ca
49. Togral G, Arıkan M, Hasturk AE, Gungor S. Painful scoliosis due to superposed giant cell bone tumor and aneurysmal bone cyst in a child. *J Pediatr Orthop B*. 2014;23(4):328-332. doi:10.1097/BPB.0000000000000055
50. Kato S, Murakami H, Demura S, et al. Patient-reported outcome and quality of life after total en bloc spondylectomy for a primary spinal tumour. *Bone Joint J*. 2014;96-B(12):1693-1698. doi:10.1302/0301-620X.96B12.33832
51. Alfawareh MD, Shah ID, Orief TI, Halawani MM, Attia WI, Almusrea KN. Pediatric upper cervical spine giant cell tumor: case report. *Global Spine J*. 2015;5(4):e28-e33. doi:10.1055/s-0034-1396433
52. Finstein JL, Chin KR, Alvandi F, Lackman RD. Postembolization paralysis in a man with a thoracolumbar giant cell tumor. *Clin Orthop Relat Res*. 2006;453:335-340. doi:10.1097/01.blo.0000229304.59771.a3
53. Yang H, Im GH, Nielsen GP, Kheterpal A, Schwab JH. Primary thoracic giant cell tumor of bone sensitive to steroids. *Skeletal Radiol*. 2018;47(10):1431-1435. doi:10.1007/s00256-018-2911-y
54. Xu K, Wan W, Li B, et al. Prognostic significance of preoperative plasma d-dimer level and clinical factors in patients with spinal giant cell tumor: retrospective analysis of 153 patients in a single center. *World Neurosurg*. 2019;122:e872-e880. doi:10.1016/j.wneu.2018.10.169
55. El Haddad A, Bassou D, Chaouir S, Amil T, Hanine A. Rare lumbar spine localization of a giant cell tumor [in French]. *J Radiol*. 2011;92(7-8):732-734. Localisation rare d'une tumeur a cellules geantes au niveau du rachis lombaire. doi:10.1016/j.jradio.2011.05.005
56. Law GW, Yeo NEM, Howe TS, Tan YZ, Tan SB, Siddiqui MMA. Recommencement of denosumab for unresectable giant cell tumor of the cervical spine: a case report. *Spine (Phila Pa 1976)*. 2018;43(9):E551-E556. doi:10.1097/BRS.0000000000002440
57. Gille O, Oliveira Bde A, Guerin P, Lepreux S, Richez C, Vital JM. Regression of giant cell tumor of the cervical spine with bisphosphonate as single therapy. *Spine (Phila Pa 1976)*. 2012;37(6):E396-E399. doi:10.1097/BRS.0b013e31823ed70d
58. Nakazawa T, Inoue G, Imura T, et al. Remarkable regression of a giant cell tumor of the cervical spine treated conservatively with denosumab: a case report. *Int J Surg Case Rep*. 2016;24:22-25. doi:10.1016/j.ijscr.2016.05.008
59. Pannu CD, Kandhwal P, Raghavan V, Khan SA, Rastogi S, Jayaswal A. Role of bisphosphonates as adjuvants of surgery in giant cell tumor of spine. *Int J Spine Surg*. 2018;12(6):695-702. doi:10.14444/5087



60. Kinoshita H, Orita S, Yonemoto T, et al. Successful total en bloc spondylectomy of the L3 vertebra with a paravertebral giant cell tumor following preoperative treatment with denosumab: a case report. *J Med Case Rep.* 2019;13(1):116. doi:10.1186/s13256-019-2029-4
61. Zhou H, Jiang L, Wei F, et al. Surgical approach selection for total spondylectomy for the treatment of giant cell tumors in the lumbar spine: a retrospective analysis of 12 patients from a single center. *Asia Pac J Clin Oncol.* 2018;14(2):e103-e108. doi:10.1111/ajco.12767
62. Mattei TA, Ramos E, Rehman AA, Shaw A, Patel SR, Mendel E. Sustained long-term complete regression of a giant cell tumor of the spine after treatment with denosumab. *Spine J.* 2014;14(7):e15-e21. doi:10.1016/j.spinee.2014.02.019
63. Swanger R, Maldjian C, Murali R, Tenner M. Three cases of benign giant cell tumor with unusual imaging features. *Clin Imaging.* 2008;32(5):407-410. doi:10.1016/j.clinimag.2007.12.003
64. Inoue G, Imura T, Miyagi M, et al. Total en bloc spondylectomy of the eleventh thoracic vertebra following denosumab therapy for the treatment of a giant cell tumor. *Oncol Lett.* 2017;14(4):4005-4010. doi:10.3892/ol.2017.6655
65. Al-Shamary E, Al-Dhafeeri W, Al-Sharydah A, Al-Suhibani S, Kussaibi H, Al-Issawi W. Total spondylectomy for upper thoracic spine giant cell tumor: a case report. *Case Rep Oncol.* 2019;12(1):131-138. doi:10.1159/000497379
66. Takeda N, Kobayashi T, Tandai S, et al. Treatment of giant cell tumors in the sacrum and spine with curettage and argon beam coagulator. *J Orthop Sci.* 2009;14(2):210-214. doi:10.1007/s00776-008-1299-2
67. Campanacci M, Baldini N, Boriani S, Sudanese A. Giant-cell tumor of bone. *J Bone Joint Surg Am Vol.* 1987;69(1):106-114.
68. Niu X, Zhang Q, Hao L, et al. Giant cell tumor of the extremity: retrospective analysis of 621 Chinese patients from one institution. *J Bone Joint Surg Am.* 2012;94(5):461-467. doi:10.2106/JBJS.J.01922
69. Hudson TM, Schiebler M, Springfield DS, Enneking WF, Hawkins IF, Spanier SS. Radiology of giant cell tumors of bone: computed tomography, arthro-tomography, and scintigraphy. *Skeletal Radiol.* 1984;11(2):85-95.
70. Murphey MD, Nomikos GC, Flemming DJ, Gannon FH, Temple HT, Kransdorf MJ. From the archives of AFIP. Imaging of giant cell tumor and giant cell reparative granuloma of bone: radiologic-pathologic correlation. *Radiographics.* 2001;21(5):1283-1309.